EIGHTEENTH EUROPEAN ROTORCRAFT FORUM

BU - 07

Paper N° 71

CALCULATION OF THE STEADY ROTOR FLOW USING AN OVERLAPPING EMBEDDED GRID TECHNIQUE

R. STANGL
S. WAGNER
UNIVERSITÄT STUTTGART

SEPTEMBER 15-18, 1992

AVIGNON, FRANCE

ASSOCIATION AERONAUTIQUE ET ASTRONAUTIQUE DE FRANCE

CALCULATION OF THE STEADY ROTOR FLOW USING AN OVERLAPPING EMBEDDED GRID TECHNIQUE

Dipl. Ing. R. Stangl
Prof. Dr-Ing. S. Wagner
Institut für Aerodynamik und Gasdynamik
Universität Stuttgart

Abstract

An existing explicit or implicit 3-D Euler Method for the calculation of the flow field around a helicopter rotor in hover was prepared for the application of a new grid technique, which allows the treatment of very complex configurations and of arbitrary blade motions with minimized effort.

1. Introduction

The single block grids, used up to now with the existing Euler codes, have proved their capabilities calculating the rotor flow including transonic effects, tip vortex and wake capturing. But they reach their limits, if more complex configurations are examined (e.g. a helicopter fuselage, a tail rotor,...) or, for unsteady calculations, arbitrary blade motions are introduced. In the second case, for example, in principle a new grid must be generated at each time step, if a fixed outer boundary is recommended. Additionally the relative cell velocity and the alteration of the cell volumes must be stored for each cell.

Current research efforts aim to circumvent such problems with methods such as domain decomposition or unstructured grids.

At a **domain decomposition technique** the flow domain is divided into sub domains, which accept easily constructed grids. In addition to the multiblock method, grid patching (or zonal method) and grid overlapping are the two widely used methods of domain decomposition.

The **zonal methods** require the domain to be divided in sub domains where the grids are patched together along common boundaries.

The **grid overlapping method** (or **embedded grids method**) does not require such common boundaries but common regions to provide the means of matching the solutions between sub domains. One sub domain can be completely or partially embedded within another. The computation is separately done in each grid, and the flow variables are interchanged as boundary conditions in defined zones. One benefit is the possible treatment of very complex configurations by simply adding new grids. But in our case the main advantage is the introduction of arbitrary blade motions by calculating and storing only the relative motions of the grids.

2. Baseline solution algorithm

The governing equations of the baseline solution algorithm are the Euler-Equations formulated in a blade fitted, rotating coordinate system.

$$\vec{\Phi} + \vec{E}_x + \vec{F}_y + \vec{G}_z = -\vec{K}$$

with

$$\Phi = \begin{pmatrix} \rho \\ \rho\bar{u} \\ \rho v \\ \rho w \\ \rho\bar{e} \end{pmatrix} \quad E = \begin{pmatrix} \rho u \\ \rho\bar{u}u \\ \rho v u \\ \rho w u \\ \rho\bar{h}u - p\omega r \end{pmatrix} \quad F = \begin{pmatrix} \rho v \\ \rho\bar{u}v \\ \rho v^2 + p \\ \rho w v \\ \rho\bar{h}v \end{pmatrix} \quad G = \begin{pmatrix} \rho w \\ \rho\bar{u}w \\ \rho v w \\ \rho w^2 + p \\ \rho\bar{h}w \end{pmatrix} \quad K = \begin{pmatrix} v \\ 2v\bar{u} \\ v^2u^2 \\ vw \\ v\bar{h} \end{pmatrix}$$

The method used is a finite volume approach that bases on characteristical flux averaging and is developed by Eberle [1] and further developed to be applied to rotor flow by Wagner, Hertel, Krämer [2,3,4,5,6,7]. An implicit iterative relaxation method is used for convergence acceleration. For hovering rotors the method has proven the accurate modelling of all relevant physical effects. It is intended to extend the code for unsteady calculations in the future.

3. Overlapping Embedded Grid Technique

The overlapping and embedded grid method implemented is called Chimera scheme and was first introduced 1983 by Steger and Benek [8] and was applied on 3-dimensional configurations by Baysal, Fouladi and Lessard [9].

The elements of an overlapping embedded grid method are:

Conventional **grid generation** for the sub domains. In our case two different grids are involved: First the `Body-grid`, which covers the region near the rotor, and second the `Cover-grid`, which encloses the whole flow region including the rotor with its body-grid.

A **hole procedure** to indicate regions that are computed with more than one grid and to mark the cells in which the solutions are transferred from the other grids. The method used is derived from a method first introduced by Steger and Benek [8].

The information transfer between the sub domains called **updating** herein.

A **flow solver** that is adapted on the method.

3.1. Grid generation

3.1.1. Body grid

The 'Body-grid' is a conventional O-O type mesh and is derived from the single block grid generation method used with our flow solver. It is generated by a differential method and solves a system of higher order differential equations. The solution algorithm is simple and requires only the boundary conditions. The distribution of the grid points is very smooth and easy to influence only with a variation of a few parameters.

The algorithm applied here bases on a system of elliptical partial differential equations called **Poisson-equations**.

$$
\begin{aligned}
X_{\xi\xi} + X_{\eta\eta} + X_{\zeta\zeta} &= P \\
Y_{\xi\xi} + Y_{\eta\eta} + Y_{\zeta\zeta} &= Q \\
Z_{\xi\xi} + Z_{\eta\eta} + Z_{\zeta\zeta} &= R
\end{aligned}
$$

where X, Y, Z are the requested co-ordinates, ξ , η and ζ are the curvilinear co-ordinates and P, Q, R are called source terms. They are again determined with a system of PDE´s called **Laplace-equations**.

$$
\begin{aligned}
P_{\xi\xi} + P_{\eta\eta} + P_{\zeta\zeta} &= 0 \\
Q_{\xi\xi} + Q_{\eta\eta} + Q_{\zeta\zeta} &= 0 \\
R_{\xi\xi} + R_{\eta\eta} + R_{\zeta\zeta} &= 0
\end{aligned}
$$

One obtains a fourth order, decoupled equation system, which can be solved iteratively. Details are given by Schwarz [10].

The first calculations are done with a grid with 128 grid points in I-direction, 35 in J-direction and 17 in K-direction (Figure 1).

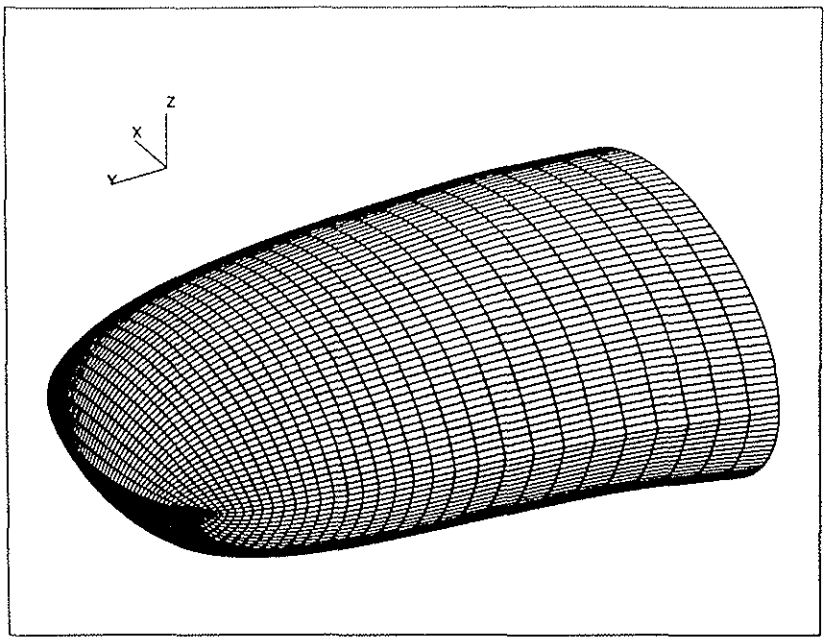

Figure 1 Body grid derived from conventional O grid

For the next investigations a grid with a new far field shape will be introduced (Figure 2). This far field will be better suited for the special requirement of this method.

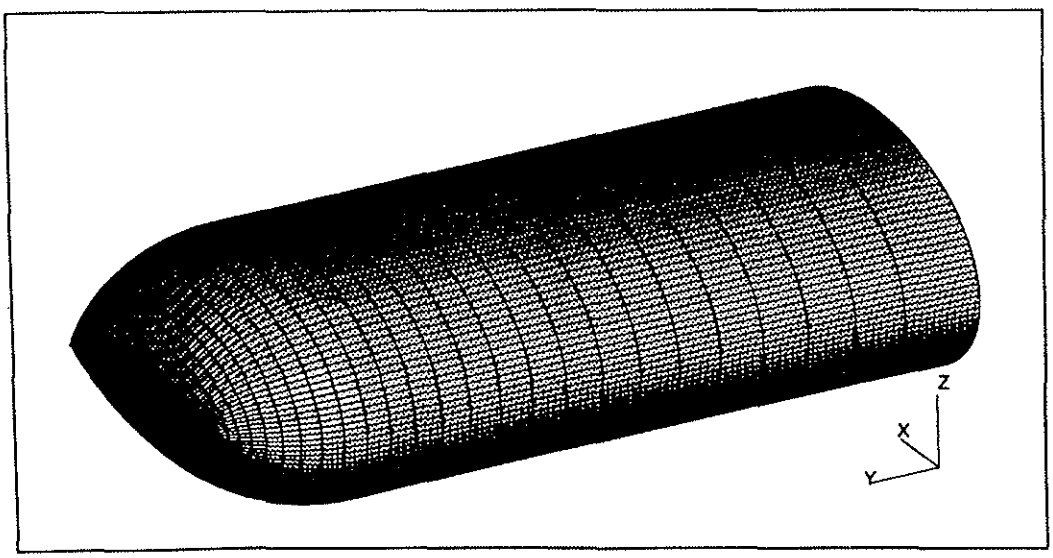

Figure 2 Outer boundary of new body grid

Since the volume ratio between the grid cells of the cover- and body-grid will have a great effect on the accuracy of the updating, there will be some investigations influencing the volume of the outer cells of the body-grid.

3.3.2. Cover grid

There are two different mesh types in use. One has a simple cylindrical co-ordinate structure, where it is possible to cluster grid points in regions with high solution gradients (Figure 3). The grid shown has 35 grid points in I-direction, 35 grid points in J-direction and 35 grid points in K-direction.The other cover grid has a cartesian co-ordinate structure with equivalent options clustering the grid points.

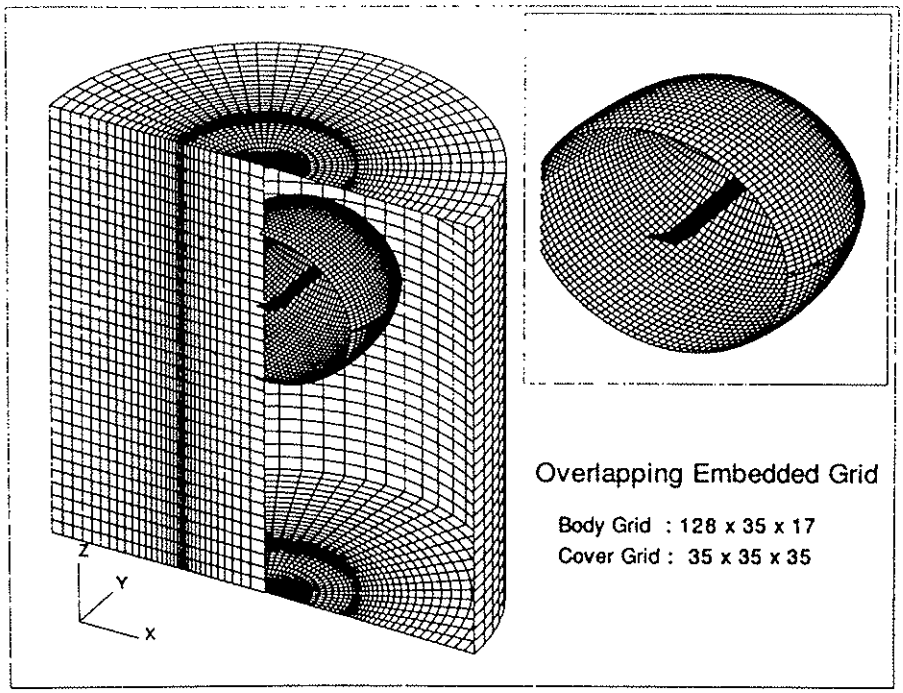

Figure 3 Cylindrical cover grid with body grid and rotor

These structures were chosen because of some advantages. First the grid generation is very fast, second the clustering of grid points in defined zones can be done by a short algorithm, and third one can identify the cell, which covered a certain point of the body grid, with minimal effort.

3.2. Hole procedure

As a result of over lapping, some cells of the cover grid lie inside a defined K-level of the body grid. But it is neither computationally economical nor desirable for the overall accuracy to compute these so called 'hole cells' twice. In addition, the cells of the cover grid, which abut on the hole cells, must be marked, because they are needed for the updating. Hence, a search method is used to create and locate the hole in the cover grid.

This search procedure may be explained briefly:

1. Specification of an initial hole boundary as a defined K-level surface K_T of the body-grid

The following steps are applied for each net plane with constant J-index (cylindrical surfaces)

2. Determination of the cells Z_{CH} of the level K_T of the body-grid that lie inside the cell row of the cover grid with constant J-index (Figure 4).

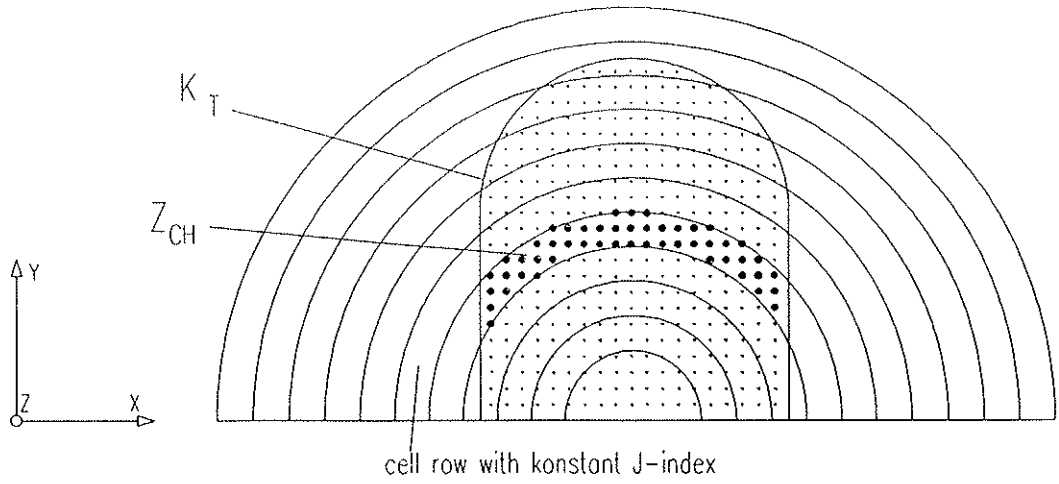

Figure 4

3. Calculation of a temporary origin P_0 of the hole

$$\overline{P_0} = \frac{1}{n} \cdot \sum_{1}^{n} \overline{Z_c},$$

where $\overline{P_0}$ and $\overline{Z_c}$ are the coordinates of the origin and the cells

and n are the number of cells

4. Determination of the maximum distance D_{max} of the cells Z_C to the temporary origin P_0. (Figure 5).

5. Searching the cells of the cover grid,which have a distance to D_0 smaller than D_{max}. (which lie inside the search circle (Figure 5)).

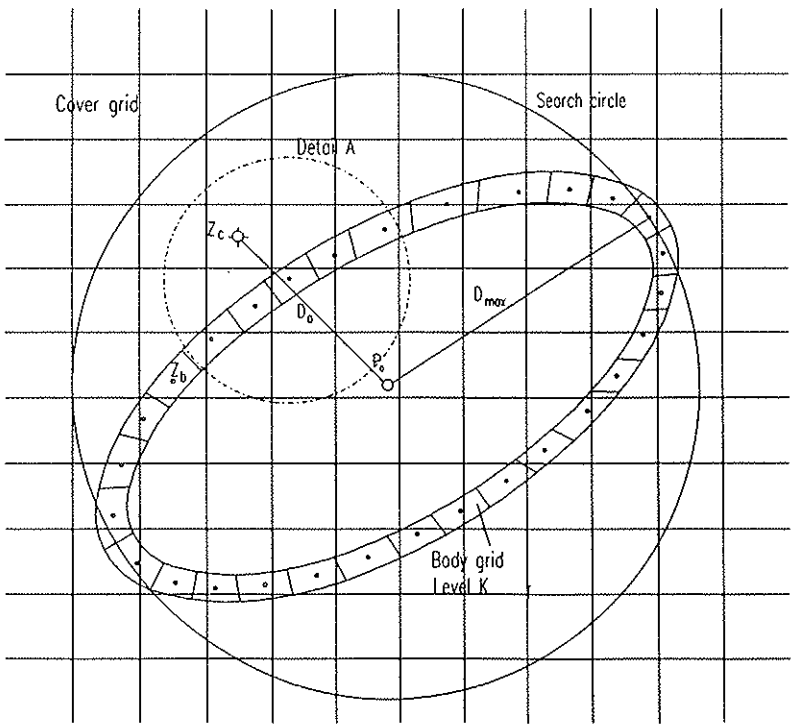

Figure 5

6. If step 5 is fulfilled, the following computations are done for these cells:

6.1. Searching the nearest cell Z_{bn} of level K_T of the body-grid (Figure 6).

6.2. Building the vector N, which is normal to the net plane K_T for this cell (Figure 6).

6.3. Building the vector V_{cb} between of Z_c and Z_{bn} (Figure 6).

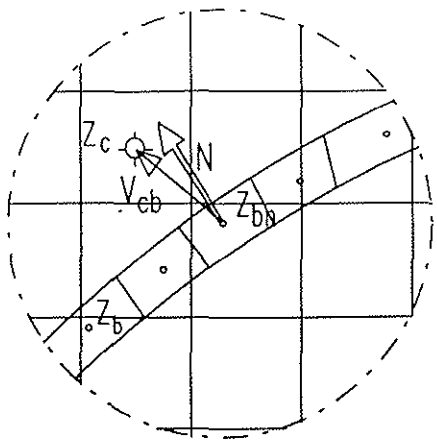

Figure 6

6.4. Building the dot-product D between the normal vector N and the vector V_{cb}.

If the dot-product D is lower than 0, the point Z_c is inside the hole and it gets an IFLAG=1, otherwise it gets an IFLAG=0.

7. Now we must mark the cells Xc of the cover-grid, which abut on the cells with IFLAG=1: If at least one neighbouring cell has an IFLAG=1, this cell gets an IFLAG=-1.

8. For a scheme that is second order accurate we need two cell rows for a boundary condition, therefore, we must mark the cells that border on the cells with IFLAG=-1.
These cells get an IFLAG=2.

The hole procedure is implemented and tested. Figure 7 shows the results of a calculation. One can see the initial hole boundary and one net plane of the cover grid with constant J-index. The different grey scales show the different values of the IFLAG.

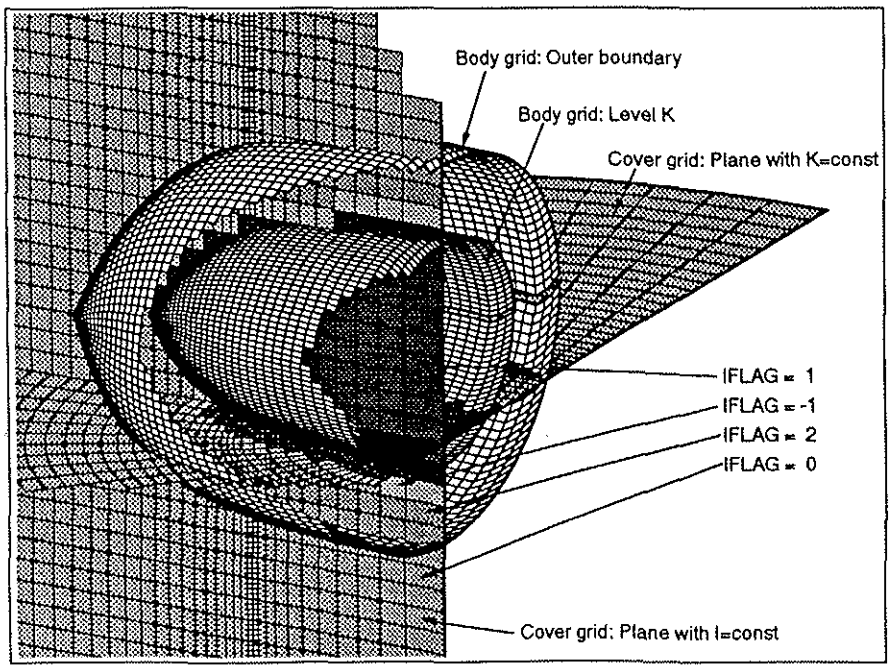

Figure 7 Results of hole procedure

3.3. Updating the Solution Variables

The **updating** can be done in various ways, but in principle these methods are not conservative. So a main objective of the future work will be the search of an appropriate method.

Up to now each cell on the outer two cell rows of the body grid gets the value of that cover grid cell in which its centre is placed. Because of the cylindrical structure of the cover grid this computation is very fast. Figure 8 shows the result of that updating. One net plane on the cover grid with a constant K-index is shown with a free chosen variable plotted. On the outer boundary of the body grid the transferred values are plotted. On detail A one can see how the structure of the cover grid influences the values on the body grid.

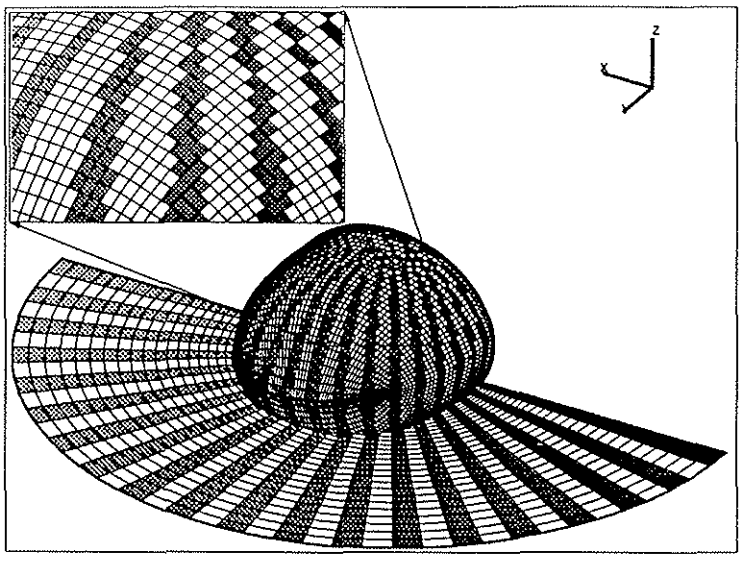

Figure 8 Updating from cover grid to body grid

The updating from the body grid to the cover grid is more expensive in CPU time. One way is the transfer of the values of the nearest body grid cell. Another tested method uses a distance weighted transfer of the nearest 2 to 8 cells of the body grid.

But surely these methods must be improved for a good final result. In Figure 9 the result of such an updating is presented. The transfer happens only on the marked cell of the cover grid.

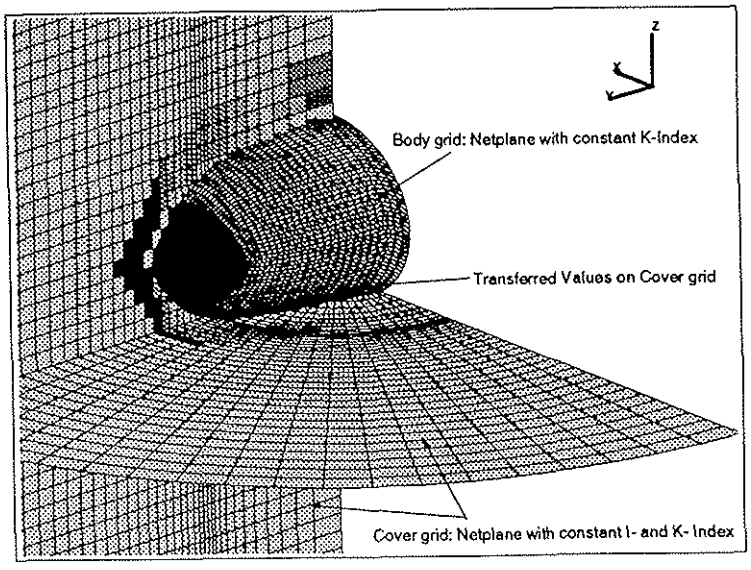

Figure 9 Updating from body grid to cover grid

This part of the overlapping embedded method will be decisive for the success and so a major part of the work will be investigated in the determination on the 'best'updating method.

4. Results

Recently, first calculations with the new method are performed.

The test cases computed base on a twobladed model rotor of Caradonna and Tung [11]. This rotor has a radius of 6 chordlenghts, a NACA 0012 profile and is untwistaed. The Mach number at the tip was 0.877 and the angle of incidence was 8 degree.

The bodygrid used has 128 grid points in I-direction, 35 grid points in J-direction and 18 grid points in K-direction. The level K_T of the hole procedure is at grid line 13 (Figure 7).

The covergrid has 40x40x70 grid points in I,J,K-direction.

In Figure 10 the z-velocity in two overlapping netplanes is plotted. The transfer from the bodygrid to the covergrid is clearly visible.

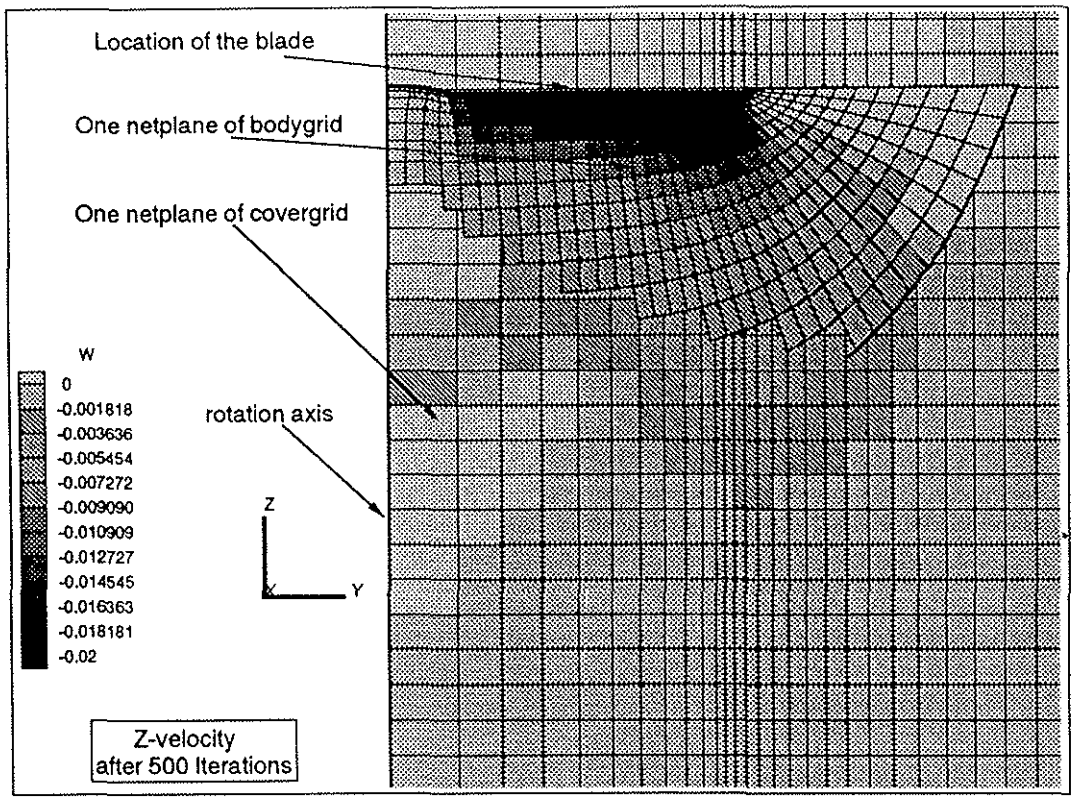

Figure 10 Z-velocity in two vertical netplanes under the rotor

Because of time restrictions only 500 Iterations were performed. The computatons are done on a IBM 550 RS 6000 Workstation. For one iteration the computer required approximately one minute CPU time.

Figure 11 shows contour lines of the density on the blade surface and the pressure coefficient c_p plotted at three different y-stations: at r/R = 0.80, r/R = 0.89 and r/R = 0.96.

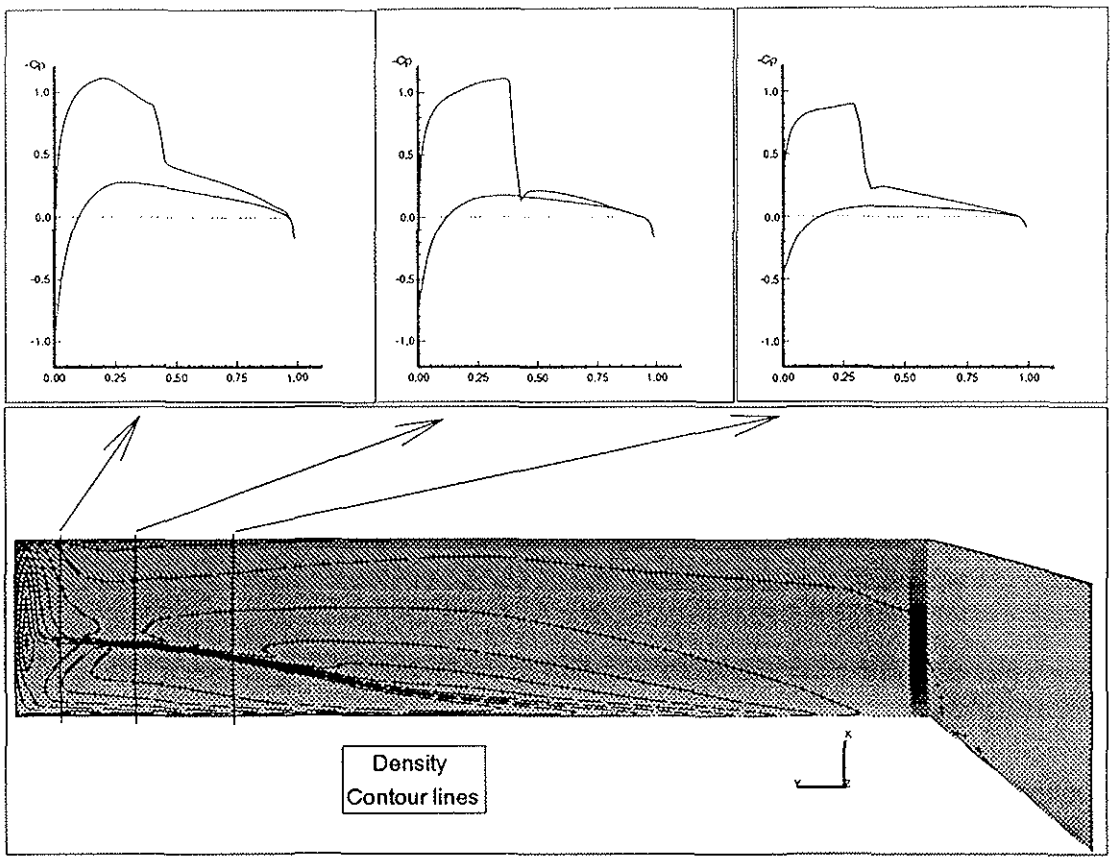

Figure 11 Contour lines of the density and pressure coefficient

Experimental data and prior computations [7] are shown in figure 12 for a comparison.

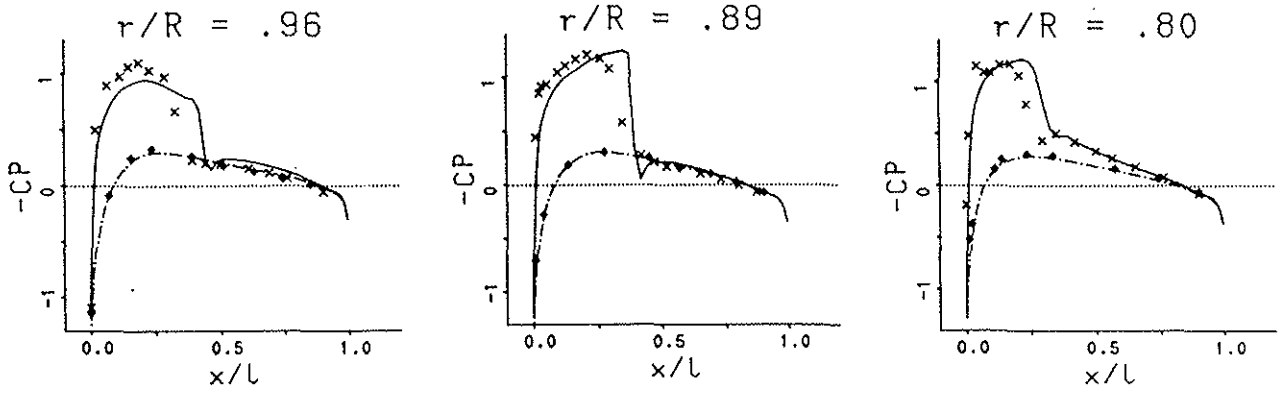

Figure 12 Results of an Euler computation compared with experimental data (from [11])

5. Conclusions

Until now only first preliminary calculations are done with the new grid technique. The results obtained are promising. But in the next months some investigations will be performed to proof the method. The following factors will be tested:

The distance between the outer boundary and the level K_T of the body grid.
Some different interpolation routines.
The difference of explicit and implicit calculations.
The influence of the different cell size in the different grids.

If it is possible to calculate the rotor flow with a satisfiing accuracy, this technique will be applicated to the extension of the code for unstady calculatons.

References

[1] A. Eberle. MBB-EUFLEX. *A New Flux Extrapolation Scheme Solving the Euler Equations for Arbitrary 3-D Geometry and Speed.* Bericht MBB/LKE122/S/PUB/140, MBB, 1984.

[2] Krämer, E., J. Hertel und S. Wagner. *A Study of the Influence of a Helicopter Rotor Blade on the Following Blades Using Euler Equations.* Paper Presented at the 14th Eurpean Rotorcraft Forum, Milano, Italy, September 20-23, 1988, Conference Proceedings, Paper No. 2.6.

[3] E. Krämer, J. Hertel and S. Wagner. *Euler procedure for calculation of the steady rotor flow with empasis on wake evolution.* In AIAA, 8th Applied Aerodynamics Conference, Portland, OR, Aug. 1990.

[4] Krämer, E., J. Hertel und S. Wagner. *Computation of Subsonic and Transonic Helicopter Rotor Flow Using Euler Equations.* Paper presented at the 13th European Rotorcraft Forum, Arles, France, September 8-11, 1987, Proceedings, Paper No. 2-14.

[5] J. Hertel, E. Krämer and S. Wagner. *Complete Euler Solution for a Rotor in Hover and a Propeller in Forward* Flight. Paper Presented at the 16th Eurpean Rotorcraft Forum, Glasgow, Scottland, 18.-21. September 1990, Proceedings, Paper No. 2.6.

[6] J. Hertel. *Euler-Lösungen der stationären Rotorströmung für Schwebe- und den axialen Vorwärtsflug mit Einbeziehung linearer Methoden.* Universität der Bundeswehr München, Dissertation an der Fakultät für Luft- und Raumfahrttechnik, 1991.

[7]E. Krämer. *Theoretische Untersuchungen der stationären Rotorblattumströmung mit Hilfe eines Euler-Verfahrens.* Universität der Bundeswehr München, Dissertation an der Fakultät für Luft- und Raumfahrttechnik, 1991.

[8] J. Steger and J. Benek. *On the Use of Composite Grid Schemes in Computational Aerodynamics.* Computer methods in applied mechanics and engeneering 64. P. 301-320. 1987

[9] O. Baysal, K. Fouladi and V. Lessard. *Multigrid and Upwind Viscous Flow Solver on Three-dimensional Overlapped and Embedded Grids.* AIAA Journal, Vol.29, No. 6, P. 903-910, June 1991.

[10] W. Schwarz. *Dreidimensionale Netzgenerierung für ein Finite Volumen Verfahren.* MBB/LKE122/S/PUB/206. 1985.

[11] F.X. Caradonna and C. Tung. *Experimental and Analytical Studies of a Model Rotor in Hover.* TM 81232, NASA, 1981.

[12] R. Stangl and, S. Wagner. *Investigations of grid manipulations.* Report 4.8.2 of BRITE EURAM Project DACRO. 1992.